Open access • Journal Article • DOI:10.1039/C3AN36866A

Rational design and synthesis of SERS labels — Source link

Yuling Wang, Sebastian Schlücker

Institutions: University of Duisburg-Essen

Published on: 18 Mar 2013 - Analyst (Analyst)

Analyst

RSC Publishing

TUTORIAL REVIEW

View Article Online
View Journal | View Issue

Rational design and synthesis of SERS labels

Cite this: *Analyst*, 2013, **138**, 2224

Yuling Wang and Sebastian Schlücker*

SERS labels are a new class of nanotags for optical detection based on Raman scattering. Central advantages include their spectral multiplexing capacity due to the small line width of vibrational Raman bands, quantification based on spectral intensities, high photostability, minimization of autofluorescence from biological specimens *via* red to near-infrared (NIR) excitation, and the need for only a single laser excitation line. Current concepts for the rational design and synthesis of SERS labels are summarized in this review. Chemical constituents of SERS labels are the plasmonically active metal colloids for signal enhancement upon resonant laser excitation, organic Raman reporter molecules for adsorption onto the metal surface for identification, and an optional protective shell. Different chemical approaches towards the synthesis of rationally designed SERS labels are highlighted, including also their subsequent bioconjugation.

Received 17th December 2012
Accepted 1st February 2013

DOI: 10.1039/c3an36866a

www.rsc.org/analyst

1 Introduction

Surface-enhanced Raman scattering (SERS) is a vibrational spectroscopic technique for probing molecules on or near the surface of metallic nanostructures, which support localized surface plasmon resonances.[1–4] Signal levels observed in SERS are typically several orders of magnitude higher than in conventional Raman scattering. The dominant contribution leading to this dramatic signal enhancement arises from the electromagnetic mechanism (EM), a purely physical effect resulting from the very strong electric fields generated upon the excitation of a localized surface plasmon resonance (LSPR).[5,6] In contrast, the so-called chemical effect is due to the interaction of the adsorbed molecules with the metal surface, which includes charge transfer resonances between the adsorbate and the metal.[7]

Dyes and molecular fluorophores are widely used labelling agents for the selective detection of biomolecules.[8] More recently, also different types of nanoparticles (NPs) have been employed as labels for conjugation to biomolecular systems (see Table 1).[9–16] In particular quantum dots are bright and stable NPs for optical detection *via* fluorescence,[9,10] while immunogold is employed for detection *via* electron microscopy.[11,12] SERS labels are relatively large (typically ~20 to 100 nm) NP labels[17–24] for the selective and sensitive optical detection of target molecules such as proteins and oligonucleotides.[25–28] In SERS NP labels/nanotags,[17–28] Raman labels/reporter molecules are permanently adsorbed onto the surface of the metal colloid (Fig. 1). The characteristic SERS signature/fingerprint generated upon laser excitation is employed for the identification of the target molecule. Direct conjugation of the biomolecules to the metal surface or to the Raman reporter molecules is one option. Generally, a shell encapsulating the SERS label (Fig. 1) is necessary for particle protection and stabilization, especially for preventing aggregation. For biological and biomedical applications, SERS labels must be conjugated to target-specific ligands such as antibodies for antigen recognition (Fig. 1).

Advantages of SERS labels over existing labelling approaches include the tremendous spectral multiplexing capacity for simultaneous target detection due to the narrow width of vibrational Raman bands; quantification using the fingerprint intensity of the corresponding SERS label; the need for only a single laser excitation wavelength to excite the Raman spectra of all SERS labels; high photostability and optimal contrast by using red to near-infrared (NIR) excitation in order to minimize the disturbing autofluorescence of cells and tissues. Examples in Sections 2 and 3 will illustrate some of these advantages. A disadvantage of SERS labels is their relatively large size and weight compared with molecular fluorophores. This is usually critical for live cell imaging, but typically not for cell surface antigens, tissue sections and assays.

The rational design of SERS labels with defined physical and chemical properties is essential for successful applications in bioanalytical chemistry and the life sciences. This review summarizes current designs of SERS labels and highlights the underlying chemical and physical concepts relevant to central parameters such as sensitivity (optical/plasmonic properties; Section 2), multiplexing and quantification (Raman reporter molecules, Section 3), stability (encapsulation/protection, Section 4), and bioconjugation (Section 5). Applications of SERS for bioanalysis, including bioassays and biomedical imaging, have been summarized recently[29–33] and will therefore not be discussed here.

Physical Chemistry, Faculty of Chemistry, University of Duisburg-Essen, Universitätsstr. 5, D-45141 Essen, Germany. E-mail: sebastian.schluecker@uni-due.de; Tel: +49 201-1836843

Table 1 Various labels for bioconjugation and the technique used for signal read-out

Label	Technique	Features	Reference
Fluorophore	Fluorescence spectroscopy	Sensitivity, multiplex capacity (~1 to 5), convenient to use	8
Enzyme	UV/Vis absorption spectroscopy	Specificity	8
Quantum dots (QDs)	Fluorescence spectroscopy	Sensitivity, multiplex capacity (~3 to 10), toxicity	9 and 10
Gold nanoparticles (immunogold)	Electron microscopy	Very high resolution	11 and 12
Gold nanoparticles	UV/Vis absorption or scattering	Enhanced visible	13 and 14
Magnetic nanoparticles	Magnetic resonance imaging	Sensitivity, small size	15 and 16
SERS labels	Raman spectroscopy	Sensitivity, multiplex capacity (~10 to 100), relatively large size	17–24

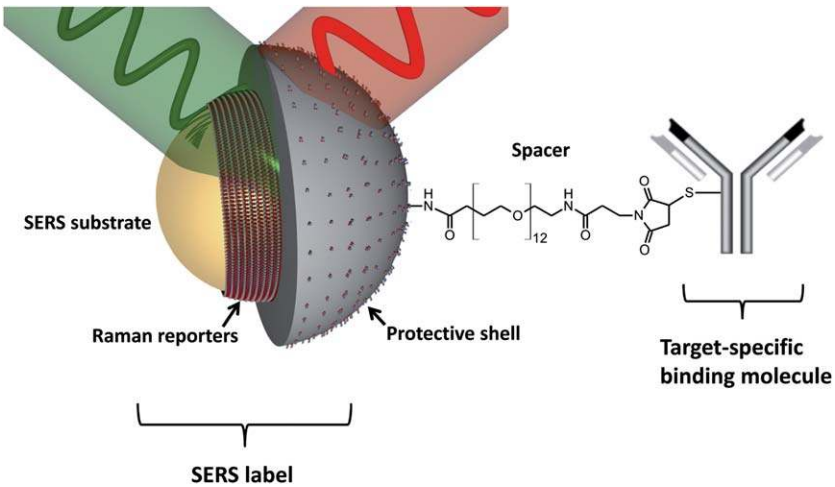

Fig. 1 Components of SERS labels: SERS substrate (plasmonically active metal colloid; here: gold NPs), Raman reporters adsorbed onto its surface (here: SAM), an optional protective layer (here: glass shell). The SERS label is conjugated to a target-specific binding molecule (here: antibody) *via* a spacer molecule. [From ref. 24.]

2 Design and synthesis of metal colloids

SERS labels (Fig. 1) contain a metal colloid for signal enhancement *via* LSPR excitation, Raman labels/reporter molecules adsorbed onto the metal surface for identification, a protective layer or shell for particle stabilization, and a ligand (*e.g.*, an antibody) for molecular recognition of the target molecule. Each chemical component of a SERS label will be discussed in this review.

The first step in the rational design of SERS labels is the choice of the metal colloid with the desired optical properties, in particular the position of the LSPR peak and the achievable signal enhancement. We will discuss the synthesis of quasi-spherical (Section 2.1) and anisotropic metal NPs (Section 2.2) as well as composite metallic NPs such as dimers and assemblies (Section 2.3), together with the description of their optical/plasmonic properties.

2.1 Synthesis of quasi-spherical metallic NPs and their optical/plasmonic properties

For an introduction to the topic of metal colloids for SERS, a recent monograph by Aroca is recommended.[1] Numerous protocols for the synthesis of metallic nanospheres are available.[34–37] The simplest and most common approach is the reduction of metal salts with a variety of reducing and capping agents. For instance, Steinigeweg and Schlücker recently reported a very simple approach for the synthesis of 20–100 nm quasi-spherical silver nanoparticles with high monodispersity.[37] Here, we highlight the preparation of Au/Ag nanoshells according to a procedure described by Xia and co-workers due to their high scattering cross sections compared with quasi-spherical solid metal NPs; the position of the LSPR depends on the size and shell thickness of the Au/Ag nanoshells and can be tuned across the Vis to NIR region.[24,38,39] First, solid silver NPs are produced in a polyol process, using silver nitrate dissolved in ethylene glycol together with polyvinylpyrrolidone (PVP) as both reducing and stabilizing agent. The silver NPs then serve as a template for the formation of hollow Au/Ag nanoshells upon addition of Au^{3+} ions. In this template-based replacement reaction, three silver atoms of the AgNPs are replaced by one gold atom: $3Ag(s) + Au^{3+}(aq) \rightarrow 3Ag^{+}(aq) + Au(s)$.[38] The shell thickness depends on the relative amount of gold added: it decreases with an increasing amount of gold, resulting in a red shift of the plasmon band.[39] In addition to these nanoshells with a solvent core and a Au/Ag shell discussed here, also

nanoshells consisting of a solid dielectric core (SiO_2) and a gold shell were produced by Halas and co-workers.[40,41] Monodisperse silica core NPs are synthesized *via* the Stöber method. After the addition of organosilanes such as 3-aminopropyltriethoxysilane, small AuNPs (1–2 nm) bind to the surface of the silica core and serve as nucleation sites for the growth of the gold shell.[40] Ag core/Au shell and Au core/Ag shell NPs are also used as SERS substrates.[42,43] Advantages include the tunability of their LSPR peaks, which can be achieved by changing the composition but without significantly changing the overall particle diameter; the surface chemistry is defined by the shell material.

The optical properties of metal NPs are important for the rational design of SERS labels; they strongly depend on the size, shape, and composition. For quantitative SERS, monodisperse metal NPs such as Ag and Au with a narrow size distribution are desired to guarantee similar scattering cross sections and therefore comparable SERS intensities.[34]

The LSPR of quasi-spherical Ag and AuNPs occurs in the blue to green region, while the LSPR of Au/Ag nanoshells can be tuned across the red to NIR region (Fig. 2, left). The position of the LSPR peak, λ_{max}, depends on a number of parameters, in particular the size of the NPs and the dielectric function of both the metal and the surrounding medium. Fig. 2 (right) shows experimental extinction spectra of quasi-spherical ~60 nm AgNPs, AuNPs and Au/Ag nanoshells in water; the corresponding LSPR peaks are observed at ~430 nm, ~540 nm and ~630 nm, respectively.

Optical excitation of the LSPR is achieved either by tuning the laser wavelength close to the LSPR peak of the colloid or by shifting the LSPR peak into resonance with a given laser wavelength. Extinction spectra recorded from metal colloids in a cuvette contain contributions from both absorption and scattering; only the latter is directly relevant for SERS.

The optical properties of spheres can be calculated using Mie theory, also called Lorenz–Mie theory.[44,45] Fig. 3 illustrates the tunability of the LSPR peak in single Au/Ag[38] and SiO_2/Au nanoshells[39] according to Mie calculations. All Au/Ag nanoshells have a radius of 27.5 nm (r_a). The shell thickness d decreases from left to right (Fig. 3, left). In contrast, the SiO_2/Au nanoshells have the same core radius of 60 nm and the thickness of the gold shell decreases from left to right (Fig. 3, right). The calculations demonstrate that the LSPR peaks of Au/Ag and SiO_2/Au nanoshells can be tuned across the entire red to NIR range.

2.2 Synthesis of anisotropic metallic nanoparticles and their plasmonic resonances

Quasi-spherical metallic NPs supporting LSPR exhibit moderate isotropic electric field enhancements. In contrast, anisotropic NPs such as rods, cubes, prisms, and nanoplates (see electron micrographs in Fig. 4) exhibit significantly higher electric field enhancements at sharp edges ("lightning rod effect"), which makes them attractive for use as plasmonic enhancers in SERS. Synthesis approaches towards various anisotropic metallic NPs are available.[46–49] One of the most widely employed approaches is seed-mediated growth, which involves seed formation and growth. So far, silver and gold nanorods,[46] branched metal nanoflowers,[50] and silver nanoplates[51] have been prepared by the seed-mediated method and used as efficient SERS substrates. Here, we highlight the synthesis of gold nanorods since their LSPR peak can be tuned by varying their size and aspect ratio. First, quasi-spherical ~4 nm gold seeds are produced by reducing gold salts with a strong reducing agent such as sodium borohydride. Subsequent reduction of more metal salt with a weak reducing agent such as ascorbic acid in the presence of structure-directing additives such as cetyltrimethylammoniumbromide (CTAB) leads to the formation of gold nanorods; the aspect ratio can be controlled by the relative concentrations of the reagents.[46]

In the polyol process, anisotropic NPs are generated by the thermal reduction of metal salts in an organic solvent with a relatively high boiling point, such as ethylene glycol (EG) or *N*,*N*-dimethylformamide (DMF), and in the presence of a polymeric stabilizer such as PVP, as reported by Liz-Marzán's group and Xia's group.[47–49] The shape of the resultant nanoparticles can be tuned by controlling the concentration of glycolaldehyde and the reaction temperature. Many of these anisotropic metal NPs can be used as plasmonic substrates for efficient generation of SERS. For example, silver nanocubes exhibiting sharp edges gave more intense SERS signals than their truncated counterparts owing to the lightning rod effect.[52]

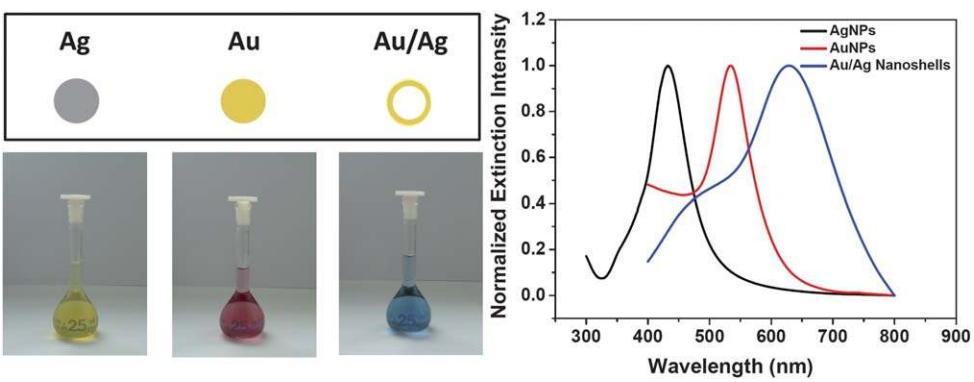

Fig. 2 Photographs (left) and experimental extinction spectra (right) of different metal nanoparticles (AgNPs, AuNPs and Au/Ag nanoshells) in water.

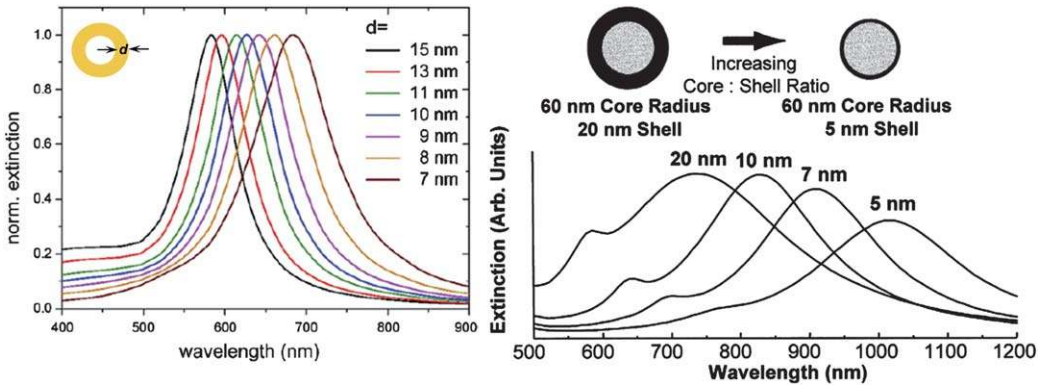

Fig. 3 (Left) Calculated extinction spectra of single Au/Ag nanoshells with a radius of 27.5 nm and varying shell thickness. (Right) Calculated extinction spectra of silica core/gold shells NPs (core radius 60 nm) with varying shell thickness. [From ref. 36, 39 and 40.]

Several groups have reported the synthesis of gold nanostars *via* seed-mediated growth by using either PVP as the capping agent in DMF[53] or CTAB as the capping agent in aqueous solution.[54] To avoid the use of CTAB and toxic DMF, Schütz *et al.* have developed a biocompatible synthesis route towards monodisperse gold nanostars (Fig. 4F) in water, with sodium citrate and hydroquinone as reducing/capping agents;[55] it was demonstrated that the as-prepared gold nanostars can be used as efficient SERS labels for tissue imaging.

The optical properties of metal NPs are strongly dependent on their shape. For gold nanorods, the optical properties can be calculated with Gans theory.[56,57] Fig. 5 depicts experimental and calculated extinction spectra of gold nanorods, in which the position of the LSPR peak strongly depends on the aspect ratio; the calculations were performed with the Gans theory and the discrete dipole approximation (DDA) method, respectively.[57] Gold nanorods have transverse and longitudinal surface plasmon resonance modes due to their anisotropy, giving rise to LSPR peaks at ~500 nm and ~600 to 700 nm, respectively (Fig. 5). With increasing aspect ratio, the LSPR peak of the longitudinal mode exhibits a red shift and a higher intensity. This tunability of the LSPR peak over the entire red to NIR range in combination with high scattering cross sections makes gold nanorods attractive for SERS.[58]

Generally, the interest in using plasmonic nanostructures as efficient SERS substrates in combination with red to NIR laser excitation is often triggered by the minimization of autofluorescence. In SERS microscopy on cells and tissue, the minimization of disturbing autofluorescence from biological specimens leads to an improved image contrast which may be more important than the maximization of absolute SERS signal levels. For optical applications *in vivo* it is additionally essential to pass through tissue such as the skin barrier, taking advantage of the "biological window" in the NIR region.

2.3 Synthesis and optical properties of metal NP clusters and assemblies

Very high electric field enhancements do not only occur at sharp tips or edges of anisotropic metal NPs, but also in the junction between two metal NPs. The extremely strong electric fields in

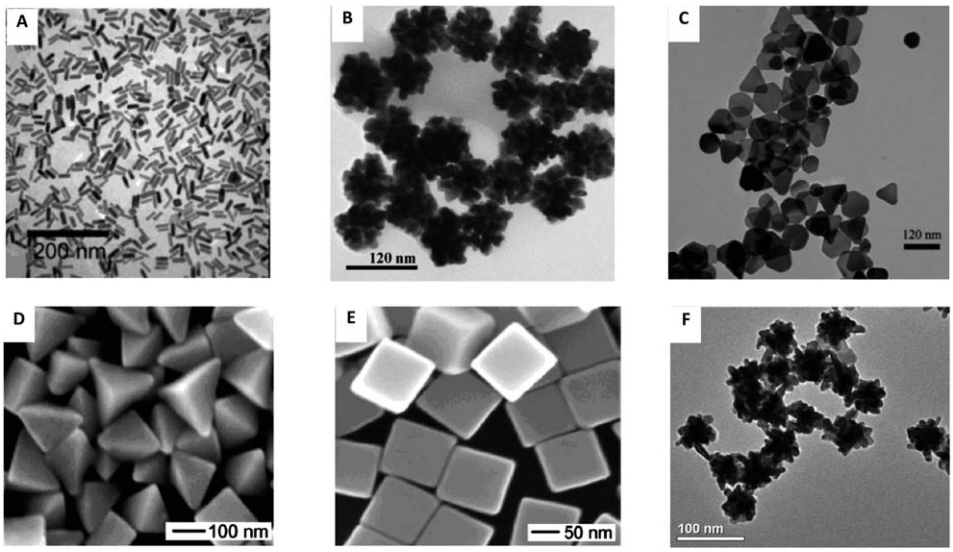

Fig. 4 Typical electron micrographs of anisotropic nanostructures for efficient SERS. Nanorods (A), nanoflowers (B), nanoplates (C), nanoprisms (D), nanocubes (E), and nanostars (F). [From ref. 46–48, 50, 51 and 55.]

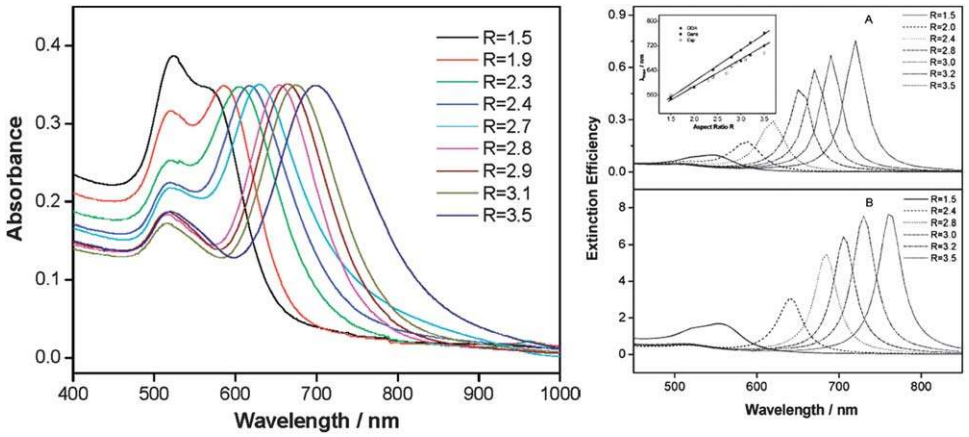

Fig. 5 Experimental (left) and calculated (right) extinction spectra of gold nanorods with tuneable plasmonic resonances. Calculations (right) are based on Gans theory (A) and the DDA method (B), respectively. [From ref. 57.]

these highly localized regions or "hot spots" arise from plasmonic coupling between two particles. The most primitive way for the fabrication of metal NP clusters is to induce particle aggregation in an uncontrolled way by centrifugation or by changing the dispersion medium or its ionic strength.[59,60] In contrast, controlled aggregation is much more difficult to achieve. Therefore, significant efforts have been made to chemically synthesize metal NPs clusters such as dimers, trimers and larger assemblies. Several methods for the controlled synthesis of dimers and assemblies of metal NPs have been developed; they have been summarized in recent reviews.[61,62]

Dimers of metal NPs are the smallest possible clusters, which exhibit a single hot spot between the two NPs upon resonant laser illumination. Important approaches towards the controlled synthesis of dimers are biomolecular directed assembly and conjugation by chemical linkers. Alivisatos and co-workers and Mirkin and co-workers have demonstrated the assembly of AuNPs into dimers, trimers and larger clusters based on a DNA-programmed procedure.[63,64] Chemical linkers such as rigid, multivalent thiol-linkers,[65] phenylacetylene,[66,67] thiol-terminated hydrophobic ligands[68] and diamines[69,70] have been demonstrated for the fabrication of dimers with a relatively high yield. To be used for efficient SERS, Xia and co-workers proposed a simple and one-step method that generates dimers without any additional assembly steps by introducing a small amount of sodium chloride into the reaction medium. The formation of dimers was achieved due to the change of the colloidal stability.[71] However, a major challenge for the synthesis of dimers is the production yield since usually only a mixture of clusters comprising monomers, dimers, trimers and larger clusters is generated.

The optical properties of dimers have been extensively investigated since the 1980s[72] and computer simulations are capable of explaining the enormous field enhancements occurring in dimers of metal NPs.[73–76] For example, Xu *et al.* reported calculations on the enhancement factor of single gold and silver NPs as well as on the corresponding dimers for different gap sizes.[74] McMahon *et al.* used the finite element method (FEM) to determine extinction spectra and electromagnetic contributions to SERS in silica-encapsulated gold dimers. For instance, the calculations confirmed the findings from Xu *et al.*,[74] namely that the EM enhancement depends critically on the particle spacing (d).[75] Sharp rises in EM enhancement were observed as d is decreased, in particular, significant changes appeared as d is decreased from 1 to 0.5 to 0.25 nm, where the maximum EM enhancement increased by three orders of magnitude. Therefore, the interparticle spacing within nanoparticle clusters is a crucial dimension for plasmonic coupling. However, for very small gaps below 1 nm, quantum mechanical effects such as tunneling must be taken into account, which can severely degrade the quality of the plasmon mode.[76]

Plasmonic nanoassemblies with multiple hot spots can also be obtained by using biomolecular/chemical linking. Kim and co-workers demonstrated the preparation of silica-encapsulated assemblies comprising a silica core and silver satellites.[77] Silica particles (~180 to 210 nm) serve as a template for the deposition of small AgNPs onto the glass surface, followed by the adsorption of Raman labels onto the metal surface of the AgNPs and subsequent encapsulation of the assembly with silica. This leads to relatively well-defined assemblies, in particular because of the monodisperse and perfectly spherical silica templates resulting from the Stöber method. Recently, Schlücker and co-workers successfully fabricated 3D plasmonic nanoassemblies *via* electrostatic self-assembly (Fig. 6a).[78] Monodisperse 80 nm gold nanospheres were incubated with Raman reporters and encapsulated with an ultrathin, ~2 to 3 nm thick silica shell and functionalized with amino groups, yielding positively charged glass-encapsulated Au cores. Negatively charged, citrate-stabilized 20 nm AuNPs were then assembled onto the surface of the Au cores *via* electrostatic attraction. TEM images of the 3D plasmonic superstructures are shown in Fig. 6b and c at high and low magnification, respectively. FEM calculations (Fig. 7) indicate that the plasmonic coupling between the core and satellite particles as well as between satellites results in the large $|E|^4$ values of up to $\sim 2 \times 10^{10}$. More recently, Xu *et al.* reported the fabrication of regiospecific plasmonic assemblies composed of gold nanorods and gold nanospheres by using DNA as the linker and it was demonstrated that the as-prepared plasmonic

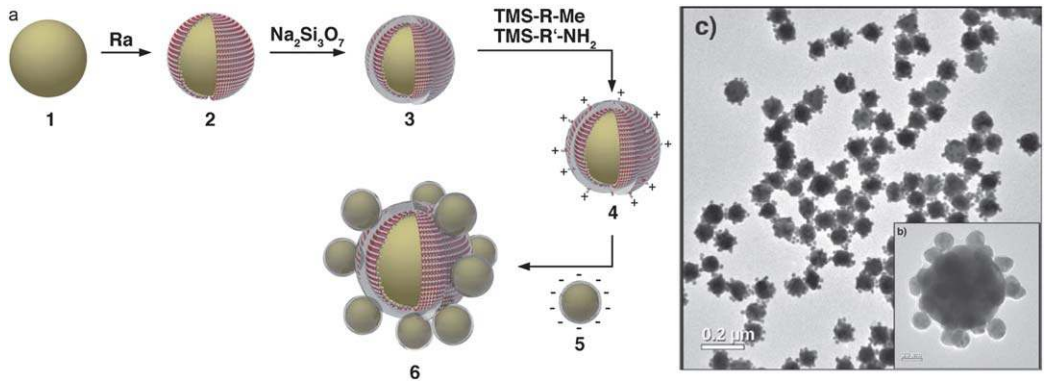

Fig. 6 (a) Synthesis of rationally designed 3D plasmonic nanostructures (**6**) *via* self assembly. 80 nm AuNPs (**1**) are coated with Raman reporters (Ra) (**2**), coated with an ultrathin silica shell (**3**), functionalized with amino groups (**4**), and finally conjugated to 20 nm AuNP satellites (**5**). (b and c) TEM images of 3D plasmonic nanostructures at high and low magnification, respectively. [From ref. 78.]

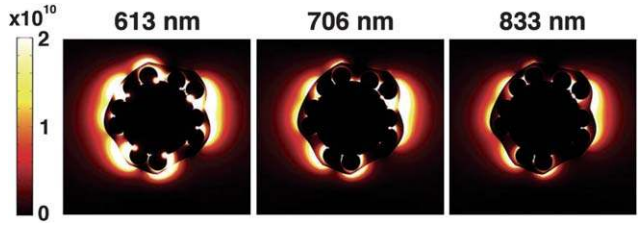

Fig. 7 Calculated spatial $|E|^4$ distribution in a 3D plasmonic superstructure for $\lambda_1 = 613$ nm, $\lambda_2 = 706$ nm and $\lambda_3 = 833$ nm. Hot spots between the core and the satellites are observed, particularly for $\lambda_1 = 613$ nm. [From ref. 78.]

nanoassemblies are efficient for *in situ* Raman imaging in live cells.[79]

Quantitative chemical, bioanalytical and life science applications of cluster/assembly-based SERS labels require the use of pure/uniform colloid samples. Separation methods are often required since usually only mixtures with different NP populations are generated (*e.g.*, different percentages of monomers, dimers, trimers and larger clusters). Different separation techniques such as chromatography,[80] size-selective precipitation,[81] capillary electrophoresis[82] and gel electrophoresis[83] have been employed. Among them, density gradient centrifugation has been shown to be very powerful for separating different cluster populations. This method was applied to NPs by Dai and co-workers for separating FeCo@C and Au nanocrystals, by carefully adjusting the density of the column material and the centrifugation speed.[84] Furthermore, Chen and co-workers achieved efficient separation of AuNPs monomers, dimers and trimers assembled from 15 nm AuNPs with high yield (95%). By using an abrupt density step and conventional centrifuge speed, the small particle clusters could be separated (Fig. 8).[85] Soon after, Schlücker and co-workers developed a fast and cost-effective purification of AuNPs in the size range of 20–250 nm by employing a multilayer quasi-continuous gradient, enabling the separation and purification of larger NPs and glass-coated clusters thereof.[86] Separation techniques will likely become more and more important for obtaining larger amounts of monodisperse, plasmonically active assemblies for quantitative and reproducible SERS.

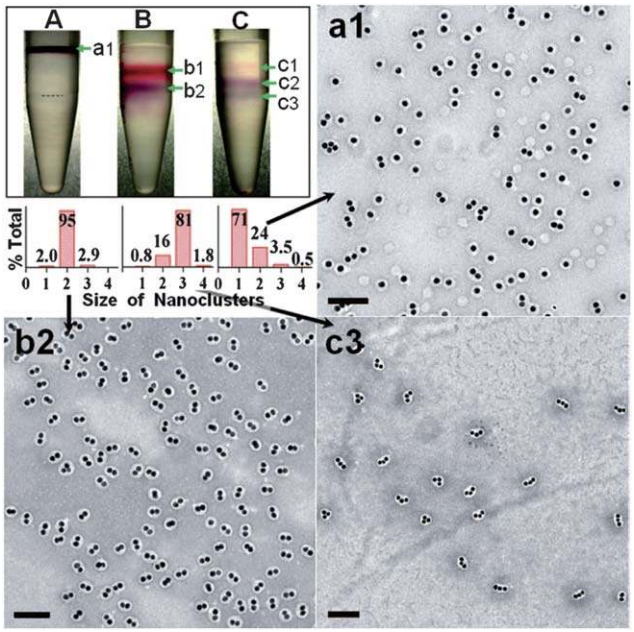

Fig. 8 Density gradient centrifugation for the separation of monomers, dimers and trimers of monodisperse AuNPs from a crude mixture of various AuNPs clusters together with the TEM images of the corresponding fractions. [From ref. 85.]

3 SERS labels: SERS nanoparticles coated with Raman labels

The second step in the design and preparation of SERS labels (Fig. 1) is the choice of Raman reporter molecules with a characteristic spectral signature. Ideal Raman labels exhibit the following properties: (i) high Raman scattering cross sections for high signal levels, (ii) a small number of atoms and/or high symmetry, leading to a minimal number of Raman bands for spectral multiplexing, (iii) low or no photobleaching for signal stability, and (iv) surface-seeking groups for chemisorption onto the metal surface.

3.1 Fluorescent dyes for SERRS and multiplexing

Fluorescent dyes adsorbed onto the surface of metallic NPs usually give rise to an extra signal enhancement (SERRS, surface

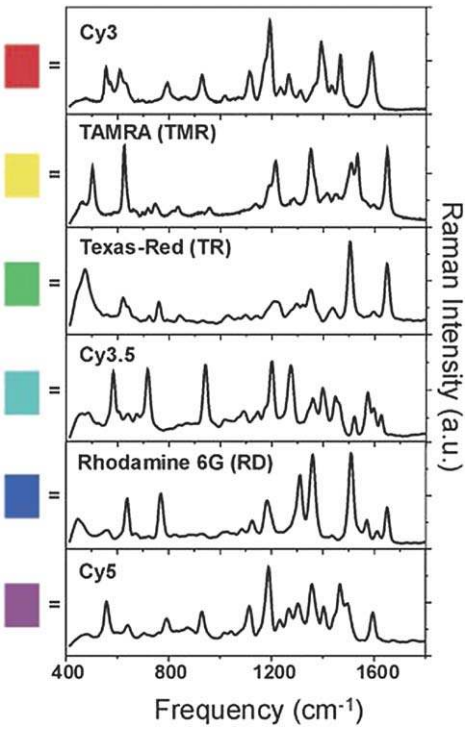

Fig. 9 Multiplexed SERRS detection with dyes as Raman reporters. [From ref. 19.]

enhanced resonance Raman scattering) compared with electronically non-resonant molecules. Spectral multiplexing is the parallel/simultaneous detection of spectrally distinct labels in a single experiment. Graham and co-workers have performed multiplexed experiments for DNA detection, using either custom-made benzotriazoles[87] or commercially available dyes including BODIPY, Cy5.5, FAM and ROX.[88–90] Mirkin and co-workers[19,21] employed commercially available dyes (Cy3, Cy3.5, Cy5, Rhodamine 6G, tetramethyl rhodamine and Texas red) as Raman labels adsorbed onto small ~13 nm AuNPs in conjunction with subsequent silver staining; the corresponding SERRS spectra are shown in Fig. 9. After bioconjugation to oligonucleotides, different DNA target sequences were detected in a microarray format with high specificity and sensitivity. More recently, Chang and co-workers reported the synthesis of NIR Raman reporters for multiplexed NIR-SERRS detection with NIR laser excitation for bioimaging with minimal interference from autofluoresences.[91–93]

3.2 SAM of Raman reporters and spectral multiplexing capacity

Compounds with functional groups such as thiols, isothiocyanates and amines are good candidates for Raman labels since they contain surface-seeking moieties for chemisorption onto the metal colloid. Porter and co-workers have introduced arylthiols/disulfides as Raman labels because they form self-assembled monolayers (SAMs) on gold surfaces *via* stable Au–S bonds.[17,20,26] Using a SAM of Raman reporter molecules has several advantages.[17,20,24,26,28] Reproducible SERS signatures are obtained due to the dense packing and uniform orientation of the Raman reporter molecules within the SAM relative to the surface normal of the metal colloid.[24,94,95] The dense packing of Raman reporter molecules within the SAM also avoids or at least minimizes unwanted spectral interferences from other molecules on the metal surface, *e.g.*, *via* adsorption from the surrounding medium. A complete monolayer with 100% surface coverage ensures maximum SERS sensitivity since it maximizes the number of Raman reporter molecules on the metal surface, in contrast to only sub-monolayer coverage (Fig. 14, left and middle). A complete/full monolayer SAM therefore leads to significantly higher SERS signals compared with sub-monolayer coverage. For instance, hollow gold/silver nanospheres covered with a complete SAM yield *ca.* 22 times

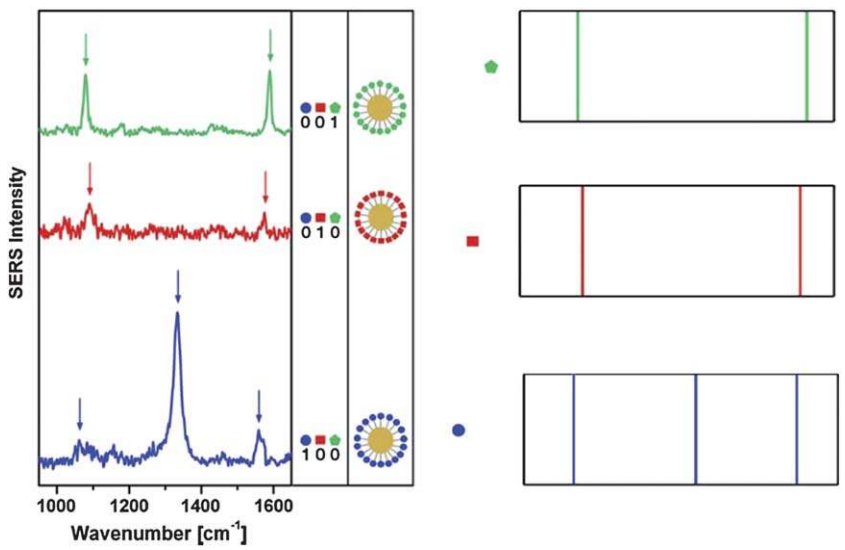

Fig. 10 SERS spectra and barcode diagram of one-component SAMs on AuNPs. [From ref. 96.]

more intense SERS signals compared with the sub-monolayer coverage upon red laser excitation (632.8 nm).[24] Spectral multiplexing can be achieved by using SAMs of Raman reporters with characteristic Raman spectra since there is little spectral overlap due to the narrow bandwidth of vibrational Raman bands. Figure 10 shows the SERS spectra of three different arylthiols (5,5′-dithiobis(2-nitrobenzoic acid), (DTNB), 2-bromo-4-mercaptobenzoic acid (BMBA) and 4-mercaptobenzoic acid (MBA)) as Raman reporters present as a complete SAM on the surface of AuNPs. In the corresponding barcode diagrams, peak positions and intensities of vibrational Raman bands are encoded in the horizontal position and width of each bar, respectively.[96]

The size and symmetry of Raman reporter molecules directly affect the number of vibrational bands. A nonlinear (linear) molecule with N atoms exhibits $3N - 6$ ($3N - 5$) vibrational bands. Smaller Raman labels are therefore beneficial for spectral multiplexing due to the smaller number of vibrational peaks. Fig. 11 shows the SERS spectra of 4-mercaptobenzoic acid (MBA) and the dye Rhodamine 6G (R6G) adsorbed onto Au/Ag nanoshells. The smaller size of MBA, which is present as a SAM on the surface of the metal colloid, leads to the appearance of only a few dominant Raman bands.[97] However, dyes such as R6G usually yield an extra enhancement *via* SERRS (as also demonstrated by Amendola and Meneghetti[98]), which is very important for sensitivity; spectrally overlapping contributions from different dyes can be differentiated by multivariate approaches.

Quantification is a further very important aspect. Various groups have demonstrated that the SERS signal response is proportional to the concentration of SERS labels[99,100] and that SERS/SERRS can quantify the concentration of DNA[90] and proteins,[101] respectively.

Isotopologues of Raman reporter molecules, which exhibit different Raman signatures primarily due to the mass effect (H/D), are particularly well suited for quantitative studies since they exhibit the same cross section and surface affinity.[100,102]

4 Protection and stabilization

Protection and stabilization of SERS labels is a prerequisite for practical applications in bioanalytical chemistry. For instance, the resulting chemical and mechanical stability of the colloid allows particle storage and prevents particle aggregation. Furthermore, desorption of Raman labels from the metal surface as well as adsorption of spectrally interfering molecules from the environment onto the surface can be eliminated or at least minimized. The encapsulant can be functionalized for subsequent bioconjugation. Overall, a protective shell usually significantly improves colloidal stability, water solubility, and biocompatibility, and provides the functional groups for further bioconjugation.

Various encapsulants are available, including hydrophilic SAMs,[94,103,104] proteins,[22] organic polymers,[105–109] and silica.[24,25,95,99,110,111] In this section, different encapsulation approaches for SERS labels will be discussed.

4.1 Hydrophilic stabilization of SAMs

The stability and water solubility of SAM-coated metal colloids usually depend on the Raman reporter molecules. Hydrophilic spacers attached to the terminus of a Raman reporter can ensure both stability and water solubility. In the rational design of SERS labels depicted in Fig. 12, the stabilization of the SAM is achieved by covalently attaching hydrophilic monoethylene glycol (MEG) units with terminal OH groups to the Raman reporters. A small portion of Raman reporter molecules is covalently conjugated to longer triethylene glycol (TEG) units with terminal COOH moieties for bioconjugation.[94] The following advantages result from this strategy: (i) maximum sensitivity due to full monolayer surface coverage; (ii) the SERS labels are water soluble due to the terminal EG spacers, independent of a particular Raman reporter; (iii) increased sterical accessibility of the SAM for bioconjugation *via* the longer TEG spacers with terminal COOH groups, and (iv) the option for controlled bioconjugation by varying the ratio of the two spacer units (MEG–OH : TEG–COOH).

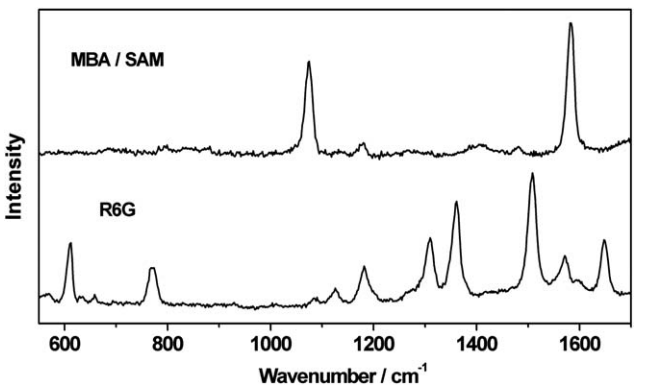

Fig. 11 SERS spectrum of MBA (SAM) in comparison with Rhodamine 6G (no SAM) adsorbed onto the surface of Au/Ag nanoshells. [From ref. 97.]

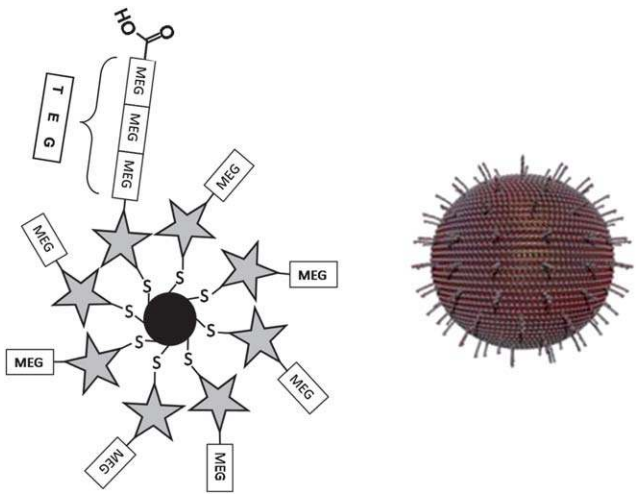

Fig. 12 Hydrophilically stabilized SERS labels for controlled bioconjugation. A complete SAM of arylthiols as Raman reporters is adsorbed onto the surface of the metal colloid. Hydrophilic mono- and triethylene glycol spacers (MEG and TEG, respectively) are conjugated to the Raman reporters and stabilize the SAM. [From ref. 94.]

A further advantage of the hydrophilic EG units is the minimization of non-specific binding.[94,103,104] This is a highly important aspect in many biological and biomedical applications: the binding selectivity is determined by the target-specific binding molecule and should not be diminished by non-specific binding of the labeling agent, which leads to false-positive results.

4.2 Stabilization by polymers including biopolymers

Stabilizing SERS labels by polymers is a widely used approach. For instance, Nie and co-workers investigated the protection of SERS labels with a layer of thiolated polyethylene glycol (PEG).[112] After addition of the Raman reporter dye, thiolated PEG was co-adsorbed onto the surface of the gold colloid in order to avoid aggregation of the colloid and enable subsequent bioconjugation. The Biomedical/Life Sciences Division of the Digital Health Group from Intel Corporation has introduced a concept for the Raman label-induced, controlled aggregation of silver NPs, which they termed COINs (composite organic–inorganic nanoparticles).[22] A shell of bovine serum albumin (BSA) protected COINs was employed for stabilization and bioconjugation.[101,113,114] Similarly, McCabe *et al.* developed a SERRS-labeled bead for encapsulating aggregates of SERRS-active NPs into a functional polymer shell for stabilization of the NPs and providing functional groups such as free carboxylates for bioconjugation.[106] Chen and co-workers developed polymer-encapsulated SERS nanoprobes by using an amphiphilic diblock copolymer (polystyrene-*block*-poly(acrylic acid)) for coating the NP surface *via* self assembly as shown in Fig. 13.[105] A central advantage is that polymer shells with a uniform thickness can easily be prepared using a one-pot synthesis. The polymer-encapsulated SERS labels provide good SERS signals and are protected against aggregation, even under harsh conditions such as high ionic strength, and against chemical oxidation.

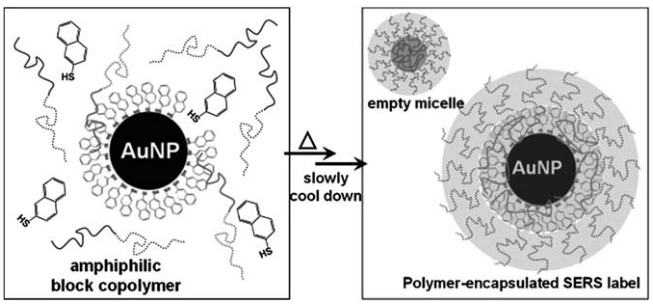

Fig. 13 Polymer-encapsulated SERS labels. [From ref. 105.]

4.3 Silica-encapsulation of SERS labels

A glass shell around a SERS label is attractive because it provides high mechanical stability and the option for long-term storage. Natan and co-workers have introduced the concept of silica encapsulation for SERS NPs[99] through co-adsorption of Raman labels and silanes (typically in a 1 : 20 stoichiometry) onto the metal NP surface. This leads to the formation of a sub-monolayer coverage with Raman reporter molecules on the metal surface as shown in Fig. 14 (middle), which is followed by silica encapsulation with a modified Stöber method.[115] Soon after, Doering and Nie presented a very similar approach towards glass-coated SERS labels.[110] Generally, a glass shell provides chemical and physical stability to the SERS labels. For example, a 20 nm thick silica shell leads to a significantly increased lifetime of gold nanocrystals in the presence of *aqua regia*: 3 h in comparison to 15 s for the bare Au colloid.[99] Further advantages are storage stability and protection against mechanical deformation.

Schlücker and co-workers have introduced the concept of silica-encapsulated SERS labels comprising a full SAM, *i.e.*, complete coverage of the metal surface with Raman reporter molecules (Fig. 14, right); this approach combines the advantages of the high chemical stability of a glass shell and the maximum and dense surface coverage of Raman labels in a full SAM for higher sensitivity.[24] Fig. 15 shows two different synthesis routes towards silica-encapsulated SERS labels comprising a full SAM.[24,95] In the first route, depicted in Fig. 15, left, the addition of Raman labels (Ra) to AuNPs leads to SAM-coated AuNPs (**1a**). Layer-by-layer deposition of poly(allylamine hydrochloride) (PAH) and polyvinylpyrrolidone (PVP) onto the SAM leads to polyelectrolyte-coated SAMs (**1b** and **1c**, respectively). The silica shell in **1d** is then formed upon addition and hydrolysis of tetraethoxyorthosilicate (TEOS) followed by condensation. This route towards silica-encapsulated SAMs (**1d**) involves several steps including different solvents and multiple centrifugation steps and is therefore labor-intensive and time consuming. In particular, it requires that the SAM is covered by a polyelectrolyte layer prior to silica encapsulation. A faster, simpler and generally applicable route towards

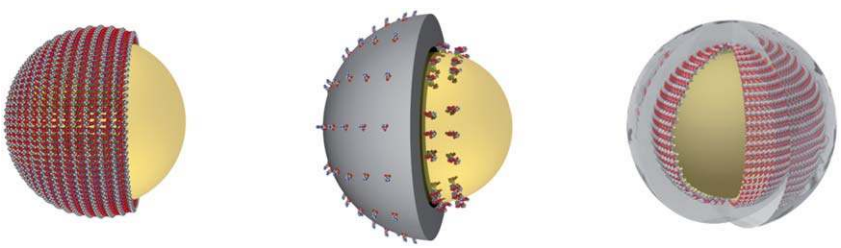

Fig. 14 SERS labels with full monolayer coverage of Raman reporters but without glass shell (left), only sub-monolayer coverage and glass shell (middle), and both full monolayer coverage and glass shell (right).

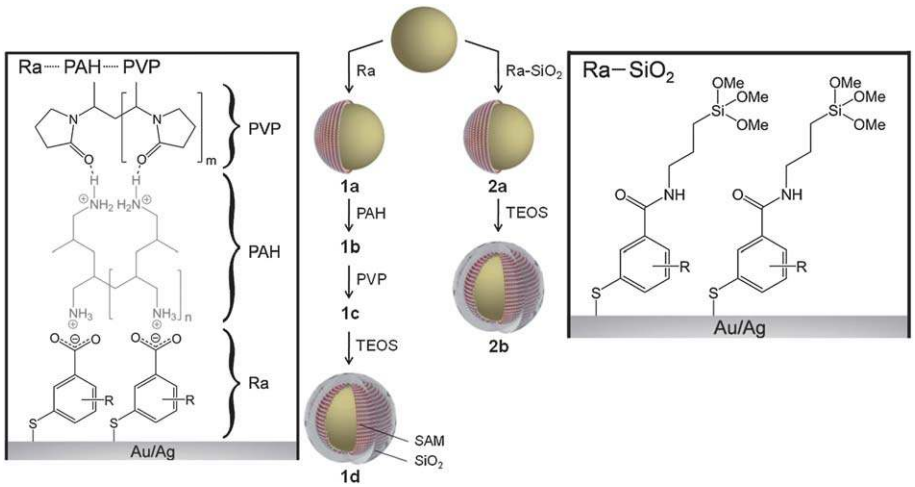

Fig. 15 Two different routes towards glass-encapsulated SERS labels containing a self-assembled monolayer (SAM) of Raman reporters on the surface of the metal nanoparticle core. Left: three-step synthesis, starting from a SAM of Raman reporter molecules (Ra) on the surface of Au/Ag nanoshells (**1a**), subsequent layer-by-layer deposition of the polyelectrolytes PAH (**1b**) and PVP (**1c**), and finally the glass encapsulation using tetraethoxyorthosilicate (TEOS) to **1d**.[16] Right: one-step approach *via* a SAM of Raman reporter molecules containing terminal SiO_2 precursors (Ra–SiO_2) (**2a**) and its direct silica encapsulation to **2b** using TEOS. [From ref. 24 and 95.]

silica-encapsulated SERS labels is possible *via* a SAM containing terminal SiO_2-precursors (Fig. 15, right): both the Raman reporter molecule (Ra) and the terminal SiO_2-precursor are covalently bound to each other (Ra–SiO_2), *i.e.*, both functions are merged into a single molecular unit.[95] In this approach, APTMS (3-amino-*n*-propyltrimethoxysilane) was covalently conjugated to mercaptobenzoic acid derivatives as Raman reporters. The addition of TEOS, its subsequent hydrolysis and condensation then led to the formation of a silica shell since the SERS labels are already vitreophilic due to the terminal SiO_2 precursor. This route towards silica-encapsulated full SAMs has the advantage that it is much faster and, more importantly, independent of the SAM's surface charge, *i.e.*, the type of a particular Raman reporter Ra in Fig. 15 top, and is therefore ideally universally applicable. However, it requires an additional organic synthesis step for obtaining the Raman reporter–SiO_2 precursor conjugate[95] (Ra–SiO_2 in Fig. 15, right). The transmission electron microscopy (TEM) images in Fig. 16 demonstrate the monodispersity of the resulting glass-encapsulated SERS labels.[24] The thickness of the glass shell can be controlled by the amount of TEOS. The 60 nm Au/Ag nanoshells in Fig. 16 have a ~10 nm (top left) and ~25 nm (bottom left and right) thick silica shell.[24] In addition to AuNPs and Au/Ag nanoshells, the silica encapsulation has also been demonstrated for a variety of other plasmonic NPs, including gold nanorods,[116] gold nanostars,[117] dimers of gold NPs,[86] aggregates,[77] and assemblies,[78] which highlights the potential of this approach.

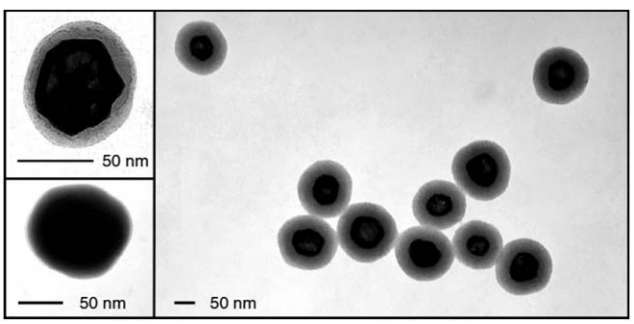

Fig. 16 Transmission electron microscopy (TEM) images of silica-encapsulated SERS labels with ~10 nm (top left) and ~25 nm (bottom left and right) thick silica shells. The diameter of the gold/silver nanoshell core is ~60 nm. [From ref. 24.]

5 Bioconjugation to SERS labels

For bioanalytical applications, SERS labels must be conjugated to ligands for target recognition (Fig. 1), *e.g.*, antibodies for antigen recognition. The ligands can be conjugated either directly to the Raman labels in the absence of a protective shell (Fig. 17, left) or to the encapsulant such as a silica shell (Fig. 17, right). In this section, we will discuss different strategies for the conjugation of biomolecules to SERS labels.

5.1 Direct conjugation of ligands to unprotected SERS labels

Direct conjugation of ligands to SERS labels can be accomplished either by electrostatic or covalent binding. For instance, adsorption of proteins to colloidal gold (immunogold) based on electrostatic forces has been explored for decades.[11,118]

An initial design of SERS labels for immunoassays by Porter and co-workers was based on the co-adsorption of antibodies and Raman labels on the surface of AuNPs as indicated in the scheme of Fig. 17 (left).[17,119] In this case, both the antibodies and the Raman reporter molecules (arylthiols) are directly co-immobilized onto the surface of the AuNPs. However, this design suffers from non-specific binding and "cross-talk" between different SERS labels.[26] Porter and co-workers continuously improved their design by covalently binding the antibodies to the Raman reporter molecules.[20] However, a drawback of this improved design is the reduced steric accessibility of the COOH moieties in the densely packed SAM on the Au surface.

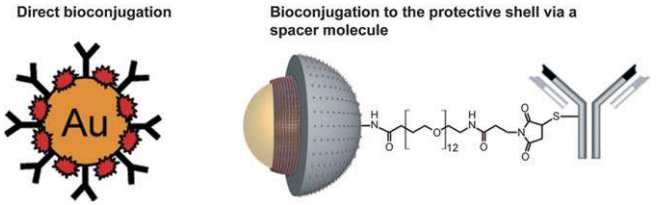

Fig. 17 Potential bioconjugation schemes for SERS labels. Left: direct bioconjugation by co-immobilization of Raman reporter molecules and antibodies onto the surface of the gold nanoparticles; right: bioconjugation of antibody *via* a spacer molecule (heterobifunctional polyethylene glycol spacer). [From ref. 24 and 119.]

Recently, Lipert, Porter and co-workers presented a further improvement by introducing the mixed monolayer approach based on two different thiols: an aromatic thiol for the generation of intense and characteristic Raman signals and an alkylthiol with a terminal functional group (*e.g.*, succinimidyl group) for bioconjugation. In addition to proteins and antibodies, oligonucleotides can also be bound directly to SERS nanoparticles for DNA detection. For example, Graham and McKenzie conjugated thiolated DNA to SERRS labels through the strong Au–S bond for DNA detection.[120]

5.2 Conjugation of ligands to protected SERS labels

a Hydrophilically stabilized SAMs. Water-soluble SERS labels stabilized by hydrophilic SAMs can be conjugated to biomolecules *via* the terminal carboxyl moieties of the longer TEG spacers (Fig. 12). After the activation of the carboxyl group by *N*-hydroxysuccinimide (NHS) and carbodiimides, the resulting NHS esters are then conjugated to primary amines, *e.g.*, from lysine residues in proteins. Antibodies directed against the protein p63 were conjugated to SERS labels with this protocol and were employed in immunohistochemistry.[55,94,121]

b Polymer-encapsulated SERS nanoprobes. Polymer-encapsulated SERS labels often provide terminal functional groups from the polymer shell. For instance, Nie and co-workers introduced AuNPs coated with thiolated PEG containing terminal carboxyl groups, to which single-chain variable fragments (scFv) could be covalently linked.[112] Overall, polymer shells can exhibit multiple terminal functional groups, which can facilitate the conjugation of SERS labels to ligands such as antibodies, oligonucleotides, *etc*. For example, McCabe *et al.* have demonstrated that dye-labelled aggregates of AgNPs encapsulated by a functional polymer can be conjugated to oligonucleotide probes and be used for the specific detection of target DNA.[106]

c Silica-encapsulated SERS nanoprobes. Bioconjugation of silica-encapsulated SERS labels typically requires the introduction of functional groups *via* silane chemistry, *e.g.*, APTMS (NH_2) or MPTMS (SH). The introduction of functional groups on the glass surface then allows bioconjugation *via* established protocols as displayed in the scheme of Fig. 17 (right). For instance, a heterobifunctional polyethylene glycol spacer was employed for both functionalization of the glass surface and subsequent bioconjugation to antibodies.[24] Widely used functional moieties are amino groups (*via* succinimides, isothiocyanates or hydrazines), carboxyl groups (*via* carbodiimides), thiol groups (*via* maleimides or acetyl bromides) and azides (*via* click chemistry).[122] Various biomolecules such as proteins, antibodies and oligonucleotides have been successfully conjugated to silica-encapsulated SERS labels for targeted research.[23,24,77,123]

Since SERS is a strongly distance-dependent effect, only the Raman label moiety close enough to the NP surface will experience the drastic electromagnetic near field enhancement and no spectral contributions from the target-specific ligands, which are spatially separated from the metal surface by the protective shell and too distant for experiencing the near-field enhancement, are observed.

6 Summary and outlook

SERS is a vibrational spectroscopic technique, which is widely used in bioanalytical chemistry and the life sciences. During the last few years, SERS labels have been developed as a novel and attractive class of biological labelling agents with unique advantages and applications that are not achievable with organic dyes or molecular fluorophores. Advantages include spectral multiplexing and quantitation in combination with high sensitivity and photostability. Significant advances in the design and synthesis of plasmonic NPs have been accomplished, including control over size and shape. In contrast, the design and synthesis of stable and well-defined 3D plasmonically active nanoassemblies with multiple hot spots for very high sensitivity still remains a challenge. For reproducibility and quantification, the use of purified colloids with a well-defined composition (no mixtures) as well as the design and synthesis of Raman reporters with similar Raman cross sections are very important.

Acknowledgements

Financial support from the Alexander von Humboldt Foundation and the German Research Foundation (DFG) is acknowledged.

References

1 R. Aroca, *Surface-Enhanced Vibrational Spectroscopy*, Wiley, New York, 2006.
2 K. Kneipp, M. Moskovits and H. Kneipp, *Surface Enhanced Raman Scattering: Physics and Applications*, Top. Appl. Phys., Springer, Berlin, 2006, vol. 103.
3 P. L. Stiles, J. A. Dieringer, N. C. Shah and R. P. Van Duyne, Surface-enhanced Raman spectroscopy, *Annu. Rev. Anal. Chem.*, 2008, **1**, 601–626.
4 *Surface-Enhanced Raman Spectroscopy: Analytical, Biophysical and Life Science Applications*, ed. S. Schlücker, Wiley-VCH, Weinheim, Germany, 2011.
5 E. C. Le Ru and P. G. Etchegoin, *Principles of Surface-Enhanced Raman Spectroscopy and Related Plasmonic Effects*, Elsevier, Amsterdam, 2009.
6 P. G. Etchegoin and E. C. Le Ru, Basic Electromagnetic Theory of SERS, in *Surface-Enhanced Raman Spectroscopy: Analytical, Biophysical and Life Science Applications*, ed. S.

Schlücker, Wiley-VCH, Weinheim, Germany, 2011, pp. 1–38.
7 A. Otto, I. Mrozek, H. Grabhorn and W. Akemann, Surface-enhanced Raman scattering, *J. Phys.: Condens. Matter*, 1992, **4**, 1143–1212.
8 J. M. Van Emon, *Immunoassay and Other Bioanalytical Techniques*, CRC Press, Boca Raton, 2007.
9 W. C. W. Chan and S. Nie, Quantum dot bioconjugates for ultrasensitive nonisotopic detection, *Science*, 1998, **281**, 2016–2018.
10 M. Bruchez Jr, M. Moronne, P. Gin, S. Weiss and A. P. Alivisatos, Semiconductor nanocrystals as fluorescent biological labels, *Science*, 1998, **281**, 2013–2016.
11 W. P. Faulk and G. M. Tayor, An immunocolloid method for the electron microscope, *Immunochemistry*, 1971, **8**, 1081–1083.
12 J. F. Hainfeld, A small gold-conjugated antibody label: improved resolution for electron microscopy, *Science*, 1987, **236**, 450–453.
13 R. Elghanian, J. J. Storhoff, R. C. Mucic, R. L. Letsinger and C. A. Mirkin, Selective colorimetric detection of polynucleotides based on the distance-dependent optical properties of gold nanoparticles, *Science*, 1997, **277**, 1078–1081.
14 R. A. Reynolds, C. A. Mirkin and R. L. Letsinger, Homogeneous, nanoparticle-based quantitative colorimetric detection of oligonucleotides, *J. Am. Chem. Soc.*, 2000, **122**, 3795–3796.
15 L. Josephson, C. H. Tung, A. Moore and R. Weissleder, High-efficiency intracellular magnetic labeling with novel superparamagnetic-Tat peptide conjugates, *Bioconjugate Chem.*, 1999, **10**, 186–191.
16 S. G. Grancharov, H. Zeng, S. Sun, S. X. Wang, S. O'Brien, C. B. Murray, J. R. Kirtley and G. A. Held, Biofunctionalization of monodisperse magnetic nanoparticles and their use as biomolecular labels in a magnetic tunnel junction based sensor, *J. Phys. Chem. B*, 2005, **109**, 13030–13035.
17 J. Ni, R. J. Lipert, G. B. Dawson and M. D. Porter, Immunoassay readout method using extrinsic Raman labels adsorbed on immunogold colloids, *Anal. Chem.*, 1999, **71**, 4903–4908.
18 D. Graham, B. J. Mallinder and W. E. Smith, Detection and identification of labeled DNA by surface enhanced resonance Raman scattering, *Biopolymers*, 2000, **57**, 85–91.
19 Y. C. Cao, R. Jin and C. A. Mirkin, Nanoparticles with Raman spectroscopic fingerprints for DNA and RNA detection, *Science*, 2002, **297**, 1536–1540.
20 D. S. Grubisha, R. J. Lipert, H.-Y. Park, J. Driskell and M. D. Porter, Femtomolar detection of prostate-specific antigen: an immunoassay based on surface-enhanced Raman scattering and immunogold labels, *Anal. Chem.*, 2003, **75**, 5936–5943.
21 Y. C. Cao, R. Jin, J.-M. Nam, C. S. Thaxton and C. A. Mirkin, Raman dye-labeled nanoparticle probes for proteins, *J. Am. Chem. Soc.*, 2003, **125**, 14676–14677.
22 X. Su, J. Zhang, L. Sun, T.-W. Koo, S. Chan, N. Sundararajan, M. Yamakawa and A. A. Berlin, Composite organic–inorganic nanoparticles (COINs) with chemically encoded optical signatures, *Nano Lett.*, 2005, **5**, 49–54.
23 C. G. Wang, Y. Chen, T. T. Wang, Z. F. Ma and Z. M. Su, Monodispersed gold nanorod-embedded silica particles as novel Raman labels for biosensing, *Adv. Funct. Mater.*, 2008, **18**, 355–361.
24 B. Küstner, M. Gellner, M. Schütz, F. Schöppler, A. Marx, P. Ströbel, P. Adam, C. Schmuck and S. Schlücker, SERS labels for red laser excitation: silica-encapsulated SAMs on tunable gold/silver nanoshells, *Angew. Chem.*, 2009, **121**, 1984–1987; *Angew. Chem., Int. Ed.*, 2009, **48**, 1950–1953.
25 W. E. Doering, M. E. Piotti, M. J. Natan and R. G. Freeman, SERS as a foundation for nanoscale, optically detected biological labels, *Adv. Mater.*, 2007, **19**, 3100–3108.
26 M. D. Porter, R. J. Lipert, L. M. Sioperko, G. Wang and R. Narayanan, SERS as a bioassay platform: fundamentals, design, and applications, *Chem. Soc. Rev.*, 2008, **37**, 1001–1011.
27 S. Schlücker and W. Kiefer, Selective Detection of Proteins and Nucleic Acids with Biofunctionalized SERS Labels, in *Frontiers in Molecular Spectroscopy*, ed. J. Laane, Elsevier, Amsterdam, 2009, pp. 267–288.
28 S. Schlücker, SERS microscopy: nanoparticle probes and biomedical applications, *ChemPhysChem*, 2009, **10**, 1344–1354.
29 J. A. Dougan and K. Faulds, Surface enhanced Raman scattering for multiplexed detection, *Analyst*, 2012, **137**, 545–554.
30 L. Rodriguez-Lorenzo, L. Fabris and R. A. Alvarez-Puebla, Multiplex optical sensing with surface-enhanced Raman scattering: a critical review, *Anal. Chim. Acta*, 2012, **745**, 10–23.
31 K. C. Bantz, A. F. Meyer, N. J. Wittenberg, H. IM, Ö. Kurtulus, S. H. Lee, N. C. Lindquist, S. H. Oh and C. L. Haynes, Recent progress in SERS biosensing, *Phys. Chem. Chem. Phys.*, 2011, **13**, 11551–11567.
32 B. H. Jun, G. Kim, M. S. Noh, H. Kang, Y. K. Kim, M. H. Cho, D. H. Jeong and Y. S. Lee, Surface-enhanced Raman scattering-active nanostructures and strategies for biosassay, *Nanomedicine*, 2011, **6**, 1463–1480.
33 Y. Zhang, H. Hong, D. V. Myklejord and W. Cai, Molecular imaging with SERS-active nanoparticles, *Small*, 2011, **7**, 3261–3269.
34 Q. Zhang, J. Xie, Y. Yu and J. Y. Lee, Monodispersity control in the synthesis of monometallic and bimetallic quasi-spherical gold and silver nanoparticles, *Nanoscale*, 2010, **2**, 1962–1975.
35 D. D. Evanoff Jr and G. Chumanov, Synthesis and optical properties of silver nanoparticles and arrays, *ChemPhysChem*, 2005, **6**, 1221–1231.
36 M. C. Daniel and D. Astruc, Gold nanoparticles: assembly, supramolecular chemistry, quantum-size-related properties, and applications toward biology, catalysis and nanotechnology, *Chem. Rev.*, 2004, **104**, 293–346.

37 D. Steinigeweg and S. Schlücker, Monodispersity and size control in the synthesis of 20–100 nm quasi-spherical silver nanoparticles by citrate and ascorbic acid reduction in glycerol–water mixtures, *Chem. Commun.*, 2012, **48**, 8682–8684.
38 Y. G. Sun, B. T. Mayers and Y. N. Xia, Template-engaged replacement reaction: a one-step approach to the large-scale synthesis of metal nanostructures with hollow interiors, *Nano Lett.*, 2002, **2**, 481–485.
39 M. Gellner, B. Küstner and S. Schlücker, Optical properties and SERS efficiency of tunable gold/silver nanoshells, *Vib. Spectrosc.*, 2009, **50**, 43–47.
40 S. J. Oldenburg, R. D. Averitt, S. L. Westcott and N. J. Halas, Nanoengineering of optical resonances, *Chem. Phys. Lett.*, 1998, **288**, 243–247.
41 S. J. Oldenburg, S. L. Westcott, R. D. Averitt and N. J. Halas, Surface enhanced Raman scattering in the near infrared using metal nanoshell substrates, *J. Chem. Phys.*, 1999, **111**, 4729–4735.
42 Y. Cui, B. Ren, J.-L. Yao, R.-A. Gu and Z.-Q. Tian, Synthesis of AgcoreAushell bimetallic nanoparticles for immunoassay based on surface-enhanced Raman spectroscopy, *J. Phys. Chem. B*, 2006, **110**, 4002–4006.
43 N. R. Jana, Silver coated gold nanoparticles as new surface enhanced Raman substrate at low analyte concentration, *Analyst*, 2003, **128**, 954–956.
44 G. Mie, *Ann. Phys.*, 1908, **25**, 377–445.
45 C. F. Bohren and D. R. Huffman, *Absorption and Scattering of Light by Small Particles*, Wiley-VCH, Weinheim, 1998.
46 C. J. Murphy, T. K. Sau, A. M. Gole, C. J. Orendorff, J. Gao, L. Gou, S. E. Hunyadi and T. Li, Anisotropic metal nanoparticles: synthesis, assembly, and optical applications, *J. Phys. Chem. B*, 2005, **109**, 13857–13870.
47 Y. Xia, Y. Xiong, B. Lim and S. E. Skrabalak, Shape-controlled synthesis of metal nanocrystals: simple chemistry meets complex physics?, *Angew. Chem.*, 2009, **121**, 62–108; *Angew. Chem., Int. Ed.*, 2009, **48**, 60–103.
48 B. J. Wiley, S. H. Im, Z. Y. Li, J. McLellan, A. Siekkinen and Y. Xia, Maneuvering the surface plasmon resonance of silver nanostructures through shape-controlled synthesis, *J. Phys. Chem. B*, 2006, **110**, 15666–15675.
49 M. Grzelczak, J. Pérez-Juste, P. Mulvaney and L. M. Liz-Marzán, Shape control in gold nanoparticles synthesis, *Chem. Soc. Rev.*, 2008, **37**, 1783–1791.
50 X.-Q. Zou, E.-B. Ying and S.-J. Dong, Seed-mediated synthesis of branched gold nanoparticles with the assistance of citrate and their surface-enhanced Raman scattering properties, *Nanotechnology*, 2006, **17**, 4758–4764.
51 X.-Q. Zou and S.-J. Dong, Surface-enhanced Raman scattering studies on aggregated silver nanoplates in aqueous solution, *J. Phys. Chem. B*, 2006, **110**, 21545–21550.
52 J. M. McLellan, A. Siekkinen, J. Chen and Y. Xia, Comparison of the surface-enhanced Raman scattering on sharp and truncated silver nanocubes, *Chem. Phys. Lett.*, 2006, **427**, 122–126.
53 S. Barbosa, A. Agrawal, L. Rodriguez-Lorenzo, I. Pastoriza-Santos, R. A. Alvarez-Puebla, A. Kornowski, H. Weller and L. M. Liz-Marzan, Tuning size and sensing properties in colloidal gold nanostars, *Langmuir*, 2010, **26**, 14943–14950.
54 C. L. Nehl, H. Liao and J. H. Hafner, Optical properties of star-shaped gold nanoparticles, *Nano Lett.*, 2006, **6**, 683–688.
55 M. Schütz, D. Steinigeweg, M. Salehi, K. Kömpe and S. Schlücker, Hydrophilically stabilized gold nanostars as SERS labels for tissue imaging of the tumor suppressor p63 by immuno-SERS microscopy, *Chem. Commun.*, 2011, **47**, 4216–4218.
56 A. Gulati, H. Liao and J. H. Hafner, Monitoring gold nanorod synthesis by localized surface plasmon resonance, *J. Phys. Chem. B*, 2006, **110**, 22323–22327.
57 H. Guo, F. Ruan, L. Lu, J. Hu, J. Pan, Z. Yang and B. Ren, Correlating the shape, surface plasmon resonance, and surface-enhanced Raman scattering of gold nanorods, *J. Phys. Chem. C*, 2009, **113**, 10459–10464.
58 C. J. Orendorff, A. Gole, T. K. Sau and C. J. Murphy, Surface-enhanced Raman spectroscopy of self-assembled monolayers: sandwich architecture and nanoparticle shape dependence, *Anal. Chem.*, 2005, **77**, 3261–3266.
59 L.-L. Sun, Y.-H. Song, L. Wang, C.-L. Guo, Y.-J. Sun, Z.-L. Liu and Z. Li, Ethanol-induced formation of silver nanoparticle aggregates for highly active SERS substrates and application in DNA detection, *J. Phys. Chem. C*, 2008, **112**, 1415–1422.
60 S. Basu, S. Pande, S. Jana, S. Bolisetty and T. Pal, Controlled interparticle spacing for surface-modified gold nanoparticle aggregates, *Langmuir*, 2008, **24**, 5562–5568.
61 L. Guerrini and D. Graham, Molecularly mediated assemblies of plasmonic nanoparticles for surface-enhanced Raman spectroscopy applications, *Chem. Soc. Rev.*, 2012, **41**, 7085–7107.
62 J. M. Romo-Herrera, R. A. Alvarez-Puebla and L. M. Liz-Marzán, Controlled assembly of plasmonic colloidal nanoparticle clusters, *Nanoscale*, 2011, **3**, 1304.
63 C. J. Loweth, W. B. Caldwell, X. Peng, A. P. Alivisatos and P. G. Schultz, DNA-based assembly of gold nanocrystals, *Angew. Chem., Int. Ed.*, 1999, **38**, 1808–1812.
64 S. Y. Park, A. K. R. Lytton-Jean, B. Lee, S. Weigand, G. C. Schatz and C. A. Mirkin, DNA-programmable nanoparticle crystallization, *Nature*, 2008, **451**, 553–556.
65 R. Sardar, T. B. Heap and J. S. Shumaker-Parry, Versatile solid phase synthesis of gold nanoparticle dimers using an asymmetric functionalization approach, *J. Am. Chem. Soc.*, 2007, **129**, 5356–5357.
66 J. P. Novak and D. L. Feldheim, Assembly of phenylacetylene-bridged silver and gold nanoparticle arrays, *J. Am. Chem. Soc.*, 2000, **122**, 3979–3980.
67 L. C. Brousseau, J. P. Novak, S. M. Marinakos and D. L. Feldheim, Assembly of phenylacetylene-bridged gold nanocluster dimers and trimers, *Adv. Mater.*, 1999, **11**, 447–449.
68 X. Wang, G. Li, T. Chen, M. Yang, Z. Zhang, T. Wu and H. Chen, Polymer-encapsulated gold-nanoparticle dimers: facile preparation and catalytical application in guided

growth of dimeric zno-nanowires, *Nano Lett.*, 2008, **8**, 2643–2647.
69 L. Guerrini, I. Izquierdo-Lorenzo, R. Rodriguez-Oliveros, J. A. Sanchez-Gil, S. Sanchez-Cortes, J. V. Garcia-Ramos and C. Domingo, α,ω-Aliphatic diamines as molecular linkers for engineering Ag nanoparticle clusters: tuning of the interparticle distance and sensing application, *Plasmonics*, 2010, **5**, 273–286.
70 L. Fabris, Bottom-up optimization of SERS hot-spots, *Chem. Commun.*, 2012, **48**, 9346–9348.
71 W. Li, P. H. C. Camargo, X. Lu and Y. Xia, Dimers of silver nanospheres: facile synthesis and their use as hot spots for surface-enhanced Raman scattering, *Nano Lett.*, 2009, **9**, 485–490.
72 P. K. Aravind, A. Nitzan and H. Metiu, The interaction between electromagnetic resonance and its role in spectroscopic studies of molecules adsorbed on colloidal particles or metal spheres, *Surf. Sci.*, 1981, **110**, 189–204.
73 J. Zuloaga, E. Prodan and P. Nordlander, Quantum description of the plasmon resonances of a nanoparticle dimer, *Nano Lett.*, 2009, **9**, 887–891.
74 H. Xu, J. Aizpurua, M. Käll and P. Apell, Electromagnetic contributions to single-molecule sensitivity in surface-enhanced Raman scattering, *Phys. Rev. E: Stat. Phys., Plasmas, Fluids, Relat. Interdiscip. Top.*, 2000, **62**, 4318–4324.
75 J. M. McMahon, A. I. Henry, K. L. Wustholz, M. J. Natan, R. G. Freeman, R. P. Van Duyne and G. C. Schatz, Gold nanoparticle dimer plasmonics: finite element method calculationsof the electromagnetic enhancement to surface-enhanced Raman spectroscopy, *Anal. Bioanal. Chem.*, 2009, **394**, 1819–1825.
76 C. E. Talley, J. B. Jackson, C. Oubre, N. K. Grady, C. W. Hollars, S. M. Lane, T. R. Huser, P. Nordlander and N. J. Halas, Surface-enhanced Raman scattering from individual Au nanoparticles and nanoparticle dimer substrates, *Nano Lett.*, 2005, **5**, 1569–1574.
77 J.-H. Kim, J.-S. Kim, H. Choi, S.-M. Lee, B.-H. Jun, K.-N. Yu, E. Kuk, Y.-K. Kim, D. H. Jeong, M.-H. Cho and Y.-S. Lee, Nanoparticle probes with surface enhanced Raman spectroscopic tags for cellular cancer targeting, *Anal. Chem.*, 2006, **78**, 6967–6973.
78 M. Gellner, D. Steinigeweg, S. Ichilmann, M. Salehi, M. Schütz, K. Kömpe, M. Haase and S. Schlücker, 3D self-assembled plasmonic superstructures of gold nanospheres: synthesis and characterization at the single-particle level, *Small*, 2011, **7**, 3445–3451.
79 L. G. Xu, H. Kuang, C. L. Xu, W. Ma, L. B. Wang and N. A. Kotov, Regiospecific plasmonic assemblies for *in situ* Raman spectroscopy in live cells, *J. Am. Chem. Soc.*, 2012, **134**, 1699–1709.
80 J. P. Wilcoxon, J. E. Martin and P. Provencio, Size distrubutions of gold nanoclusters studied by liquid chromatography, *Langmuir*, 2000, **16**, 9912–9920.
81 M. Chandler McLeod, M. Anand, C. L. Kitchens and C. B. Roberts, Precise and rapid size selection and targeted deposition of nanoparticle populations using CO_2 gas expanded liquids, *Nano Lett.*, 2005, **5**, 461–465.
82 F. K. Liu, F. H. Ko, P. W. Huang, C. H. Wu and T. C. Chu, Studying the size/shape separation and optical properties of silver nanoparticles by capillary electrophoresis, *J. Chromatogr., A*, 2005, **1062**, 139–145.
83 S. Pierrat, I. Zins, A. Breivogel and C. Sönnichsen, Self-assembly of small gold colloids with functionalized gold nanorods, *Nano Lett.*, 2007, **7**, 259–263.
84 X. M. Sun, S. M. Tabakman, W. S. Seo, L. Zhang, G. Y. Zhang, S. Sherlock, L. Bai and H. J. Dai, Separation of nanoparticles in a density gradient: FeCo@C and gold nanocrystals, *Angew. Chem., Int. Ed.*, 2009, **48**, 939–942.
85 G. Chen, Y. Wang, L. H. Tan, M. X. Yang, L. S. Tan, Y. Chen and H. Y. Chen, High-purity separation of gold nanoparticle dimers and trimers, *J. Am. Chem. Soc.*, 2009, **131**, 4218–4219.
86 D. Steinigeweg, M. Schütz, M. Salehi and S. Schlücker, Fast and cost-effective purification of gold nanoparticles in the 20–250 nm size range by continuous density gradient centrifugation, *Small*, 2011, **7**, 2443–2448.
87 D. Graham, K. Faulds and W. E. Smith, Biosensing using silver nanoparticles and surface enhanced resonance Raman scattering, *Chem. Commun.*, 2006, **42**, 4363–4371.
88 D. Graham, W. E. Smith, A. M. T. Linacre, C. H. Munro, N. D. Watson and P. C. White, Selective detection of deoxyribonucleic acid at ultralow concentrations by SERRS, *Anal. Chem.*, 1997, **69**, 4703–4707.
89 D. Graham, B. J. Mallinder and W. E. Smith, Surface-enhanced resonance Raman scattering as a novel method of DNA discrimination, *Angew. Chem.*, 2000, **112**, 1103–1105; *Angew. Chem., Int. Ed.*, 2000, **39**, 1061–1063.
90 K. Faulds, F. McKenzie, W. E. Smith and D. Graham, Quantitative simultaneous multianalyte detection of DNA by dual- wavelength surface-enhanced resonance Raman scattering, *Angew. Chem.*, 2007, **119**, 1861–1863; *Angew. Chem., Int. Ed.*, 2007, **46**, 1829–1831.
91 S. J. Cho, Y. H. Ahn, K. K. Maiti, U. S. Dinish, C. Y. Fu, P. Thoniyot, M. Olivo and Y. T. Chang, Combinatorial synthesis of a triphenylmethine library and their application in the development of surface enhanced Raman scattering (SERS) probes, *Chem. Commun.*, 2010, **46**, 722–724.
92 A. Samanta, K. K. Maiti, K. S. Soh, X. J. Liao, M. Vendrell, U. S. Dinish, S. W. Yuh, R. Bhuvaneswari, H. Kim, S. Rautela, J. Chung, M. Olivo and Y. T. Chang, *Angew. Chem., Int. Ed.*, 2011, **50**, 6089–6092.
93 K. K. Maiti, U. S. Dinish, A. Samanta, M. Vendrell, K. S. Soh, S. J. Park, M. Olivo and Y. T. Chang, Multiplex targeted *in vivo* cancer detection using sensitive near-infrared SERS nanotags, *Nano Today*, 2012, **7**, 85–93.
94 C. Jehn, B. Küstner, P. Adam, A. Marx, P. Ströbel, C. Schmuck and S. Schlücker, Water soluble SERS labels comprising a SAM with dual spacers for controlled bioconjugation, *Phys. Chem. Chem. Phys.*, 2009, **11**, 7499–7504.
95 M. Schütz, B. Küstner, M. Bauer, C. Schmuck and S. Schlücker, Synthesis of glass coated SERS nanoparticle

probes *via* SAMs with terminal SiO_2 precursors, *Small*, 2010, **6**, 733–737.
96 M. Gellner, K. Kömpe and S. Schlücker, Multiplexing with SERS labels using mixed SAMs of Raman reporter molecules, *Anal. Bioanal. Chem.*, 2009, **394**, 1839–1844.
97 S. Schlücker, in *Surface-Enhanced Raman Spectroscopy: Analytical, Biophysical and Life Science Applications*, ed. S. Schlücker, Wiley-VCH, Weinheim, Germany, 2011, p. 263.
98 V. Amendola and M. Meneghetti, Exploring how to increase the brightness of surface-enhanced Raman spectroscopy nanolabels: the effect of the Raman-active molecules and of the label size, *Adv. Funct. Mater.*, 2012, **22**, 353–360.
99 S. P. Mulvaney, M. D. Musick, C. D. Keating and M. J. Natan, Glass-coated, analyte-tagged nanoparticles: a new tagging system based on detection with surface-enhanced Raman scattering, *Langmuir*, 2003, **19**, 4784–4790.
100 S. Keren, C. Zavaleta, Z. Cheng, A. de la Zerda, O. Gheysens and S. S. Gambhir, Noninvasive molecular imaging of small living subjects using Raman spectroscopy, *Proc. Natl. Acad. Sci. U. S. A.*, 2008, **105**, 5844–5849.
101 L. Sun, K.-B. Sung, C. Dentinger, B. Lutz, L. Nguyen, J. Zhang, H. Qin, M. Yamakawa, M. Cao, Y. Lu, A. J. Chmura, J. Zhu, X. Su, A. A. Berlin, S. Chan and B. Knudsen, Composite organic–inorganic nanoparticles as Raman labels for tissue analysis, *Nano Lett.*, 2007, **7**, 351–356.
102 D. Zhang, Y. Xie, S. K. Deb, V. J. Davison and D. Ben-Amotz, Isotope edited internal standard method for quantitative surface-enhanced Raman spectroscopy, *Anal. Chem.*, 2005, **77**, 3563–3569.
103 P. A. G. Cormack, A. Hernandez-Santana, R. A. Prasath, F. McKenzie, D. Graham and W. E. Smith, Multidentate macromolecules for functionalisation, passivation and labelling of metal nanoparticles, *Chem. Commun.*, 2008, 2517–2519.
104 F. McKenzie, A. Ingram, R. Stokes and D. Graham, SERRS coded nanoparticles for biomolecular labelling with wavelength-tunable discrimination, *Analyst*, 2009, **134**, 549–556.
105 M. Yang, T. Chen, W. S. Lau, Y. Wang, Q. Tang, Y. Yang and H. Chen, Development of polymer-encapsulated metal nanoparticles as surface-enhanced Raman scattering probes, *Small*, 2009, **5**, 198–202.
106 A. F. McCabe, C. Eliasson, R. A. Prasath, A. Hernandez-Santana, L. Stevenson, I. Apple, P. A. G. Cormack, D. Graham, W. E. Smith, P. Corish, S. J. Lipscomb, E. R. Holland and P. D. Prince, SERRS labelled beads for multiplex detection, *Faraday Discuss.*, 2006, **132**, 303–308.
107 L. C. Martin, I. A. Larmour, K. Faulds and D. Graham, Turning up the light-fabrication of brighter SERRS nanotags, *Chem. Commun.*, 2010, **46**, 5247–5249.
108 A. McLintock, N. Hunt and A. W. Wark, Controlled side-by-side assembly of gold nanorods and dye molecules into polymer-wrapped SERRS-active clusters, *Chem. Commun.*, 2011, **47**, 3757–3759.
109 G. Chen, Y. Wang, M. Yang, J. Xu, S. J. Goh, M. Pan and H. Chen, Measuring ensemble-averaged surface-enhanced Raman scattering in the hotspots of colloidal nanoparticle dimers and trimers, *J. Am. Chem. Soc.*, 2010, **132**, 3644–3645.
110 W. E. Doering and S. Nie, Spectroscopic tags using dye-embedded nanoparticles and surface-enhanced Raman scattering, *Anal. Chem.*, 2003, **75**, 6171–6176.
111 X. Liu, M. Knauer, N. P. Ivleva, R. Niessner and C. Haisch, Synthesis of core–shell surface-enhanced Raman tags for bioimaging, *Anal. Chem.*, 2010, **82**, 441–446.
112 X. Qian, X.-H. Peng, D. O. Ansari, Q. Yin-Goen, G. Z. Chen, D. M. Shin, L. Yang, A. N. Young, M. D. Wang and S. Nie, *In vivo* tumor targeting and spectroscopic detection with surface-enhanced Raman nanoparticle tags, *Nat. Biotechnol.*, 2008, **26**, 83–90.
113 B. Lutz, C. E. Dentinger, L. N. Nguyen, L. Sun, J. Zhang, A. N. Allen, S. Chan and B. S. Knudsen, Spectral analysis of multiplex Raman probe signatures, *ACS Nano*, 2008, **2**, 2306–2314.
114 C. M. Shachaf, S. V. Elchuri, A. L. Koh, J. Zhu, L. N. Nguyen, D. J. Mitchell, J. Zhang, K. B. Swartz, L. Sun, S. Chan, R. Sinclair and G. P. Nolan, A novel method for detection of phosphorylation in single cells by surface enhanced Raman scattering (SERS) using composite organic–inorganic nanoparticles (COINs), *PLoS One*, 2009, **4**, 1–12.
115 W. Stöber, A. Fink and E. Bohn, Controlled growth of monodisperse silica spheres in the micron size range, *J. Colloid Interface Sci.*, 1968, **26**, 62–69.
116 C. G. Wang, Y. Chen, T. T. Wang, Z. F. Ma and Z. M. Su, Monodispersed gold nanorod-embedded silica particles as novel Raman labels for biosensing, *Adv. Funct. Mater.*, 2008, **18**, 355–361.
117 M. Li, J. Zhang, S. Suri, L. J. Sooter, D. Ma and N. Wu, Detection of adenosine triphosphate with an aptamer biosensor based on surface-enhanced Raman scattering, *Anal. Chem.*, 2012, **84**, 2837–2842.
118 *Colloidal Gold: Principles, Methods, and Applications*, ed. M.A. Hayat, Academic Press, San Diego, 1989, vol. 1–3.
119 G. Wang, H. Y. Park, R. J. Lipert and M. D. Porter, Mixed monolayers on gold nanoparticle labels for multiplexed surface-enhanced Raman scattering based immunoassays, *Anal. Chem.*, 2009, **81**, 9643–9650.
120 F. McKenzie and D. Graham, Controlled assembly of SERRS active oligonucleotide–nanoparticles conjugates, *Chem. Commun.*, 2009, 5757–5759.
121 S. Schlücker, M. Salehi, G. Bergner, M. Schütz, P. Ströbel, A. Marx, I. Petersen, B. Dietzek and J. Popp, Immuno-surface-enhanced coherent anti-stokes Raman scattering microscopy: immunohistochemistry with target-specific metallic nanoprobes and nonlinear Raman microscopy, *Anal. Chem.*, 2011, **83**, 7081–7085.
122 G. T. Hermanson, *Bioconjugate Techniques*, Academic Press, San Diego, 2008.
123 Y. Liang, J. L. Gong, Y. Huang, Y. Zheng, J. H. Jiang, G. L. Shen and R. Q. Yu, Biocompatible core-shell nanoparticle-based surface-enhanced Raman scattering probes for detection of DNA related to HIV gene using silica-coated magnetic nanoparticles as separation tools, *Talanta*, 2007, **72**, 443–449.

